SPUTTER METALIZATION OF WOLTER TYPE OPTICAL ELEMENTS

Anthony M. Ledger
The Perkin-Elmer Corporation
Norwalk, Connecticut 06856
Report No. 13437

July 1977
Final Report for Period June 1976 – June 1977

Prepared for
GODDARD SPACE FLIGHT CENTER
Greenbelt, Maryland 20771

1. Report No.	2. Government Accession No.	3. Recipient's Catalog No.

4. Title and Subtitle	5. Report Date
Sputter Metalization of Wolter Type Optical Elements	July 1977
	6. Performing Organization Code
7. Author(s) Anthony M. Ledger	8. Performing Organization Report No. 13437
9. Performing Organization Name and Address The Perkin-Elmer Corporation Norwalk, Connecticut 06856	10. Work Unit No.
	11. Contract or Grant No. NAS5-23581
	13. Type of Report and Period Covered Final Report June 1976 - June 1977
12. Sponsoring Agency Name and Address Goddard Space Flight Center J. Osantowski, Code 722 Greenbelt Road, Greenbelt, MD 20771	14. Sponsoring Agency Code

15. Supplementary Notes

16. Abstract

The analytical investigation of sputter metalization of Wolter type optical elements successfully concluded the following two objectives.

- An analytical task showed that the coating thickness distribution for both internal and external optical elements coated using either electron beam or sputter sources can be made uniform and will not affect the surface figure of coated elements.
- Sputtered samples of nickel, molybdenum, iridium and ruthenium deposited onto both hot and cold substrates showed excellent adhesion.

17. Key Words (Selected by Author(s))	18. Distribution Statement
See next page	

19. Security Classif. (of this report)	20. Security Classif. (of this page)	21. No. of Pages	22. Price*
UNCLASSIFIED	UNCLASSIFIED		

*For sale by the National Technical Information Service, Springfield, Virginia 22151.

17. Key Words (Selected by Author(s))

extreme ultraviolet X-ray spectral region telescopes
Wolter type 1 and 2 optical elements
metallic coating by sputtering
metallic coatings by vacuum evaporation from an
electron gun

TABLE OF CONTENTS

LIST OF ILLUSTRATIONS

PREFACE

OBJECTIVE

This study consisted of two primary objectives. The first was the prediction of thickness variations in metallic films deposited on glancing incidence telescope substrates. A parallel objective was the fabrication of metalized samples of nickel, ruthenium, molybdenum, and iridium on fused silica, Cervit and nickel substrates.

SCOPE OF WORK

This study provides a quantitative analysis of metalization procedures required for the Wolter type glancing incidence telescope designs. This analysis specifically addresses film deposition by resistive heating, electron bombardment and sputtering techniques. Quantitative determinations of the expected radial and axial thickness variations of the metal film are provided for the typical Wolter type elements.

CONCLUSIONS

The analytical task shows that coating thickness variations using electron beam, resistance, or sputter sources have insignificant influence upon the surface figure of glancing incidence telescope substrates. Sputtered samples of nickel, ruthenium, molybdenum, and iridium deposited on both hot and cold substrates show excellent adhesion.

SUMMARY OF RECOMMENDATIONS

The surface figure of both type 1 and type 2 Wolter telescope substrates can be maintained using the deposition techniques explored in this study.

SECTION I

INTRODUCTION

Telescopes designed for the extreme ultraviolet and X-ray spectral regions generally utilize optical systems of the Wolter type 1 or type 2 design (Refs. 1,2). Such mirror systems consist of cylindrical parabolic or hyperbolic reflector surfaces, both internal and external, which operate at grazing incidence. Although polished glass surfaces of this form act as efficient reflectors only at high angles of incidence, coating with a vacuum deposited metallic film allows designs operating over a broader range of incidence angles to be utilized effectively.

Metallic coatings can be deposited by sputtering, resistive heating, or by vacuum evaporation from an electron beam gun to form durable reflector coatings; however, such coatings are seldom deposited onto the internal and external surfaces of cylindrical mirrors as is required for Wolter type optics. The two types of configurations are shown schematically in Figure 1. The parabolic and hyperbolic mirrors for the type 1 system must be metalized on their internal cylindrical surfaces to achieve efficient high incidence reflectivity. The type 2 optical system consists of an internal parabolic mirror, similar in size to the type 1 optical elements, together with a small external hyperbolic mirror. In this configuration the internal parabolic surface and external hyperbolic surface must be metalized to enhance the grazing incidence reflectivity.

Metalization of type 1 optical elements has been carried out for the HEAO-B X-ray telescope program at Perkin-Elmer (Ref. 3) using a chrome/nickel film system deposited by electron beam gun evaporation techniques. This

---

1. J.D. Mangus, J.H. Underwood, Appl. Opt. 8, 95 (1969)
2. J.D. Mangus, Appl. Opt. 9, 1019 (1970)
3. HEAO-B X-Ray Telescope, Final Technical Report No. 13292, Perkin-Elmer Corporation, 17 Jan. 1977

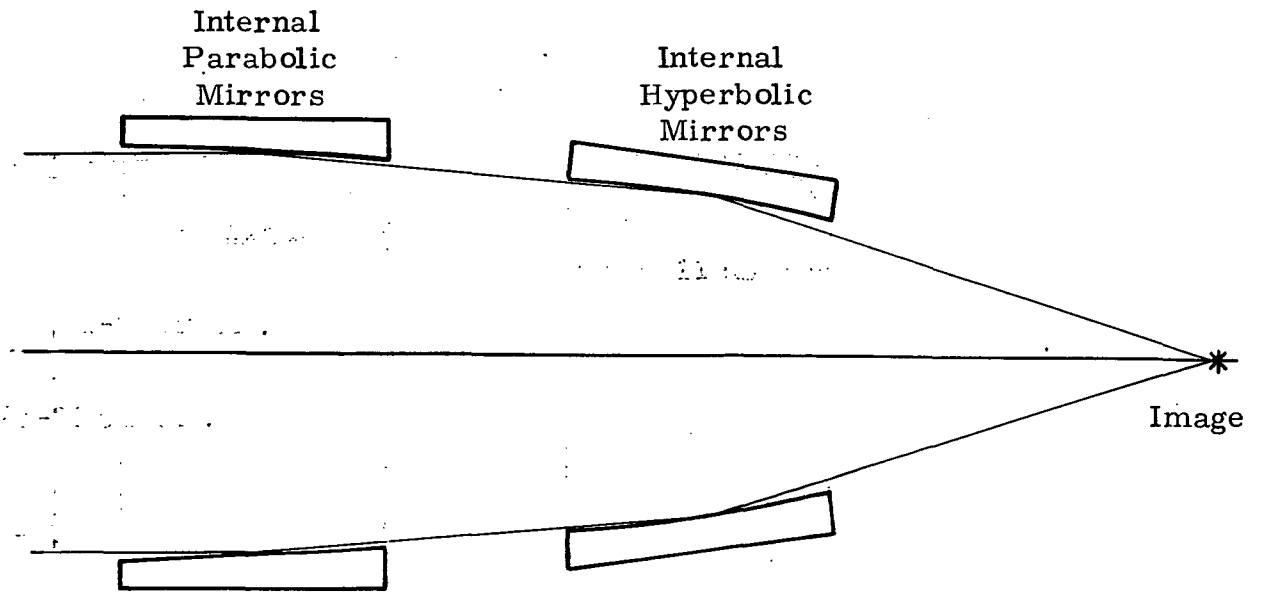

(a) Type I Wolter Telescope
For X-Ray Spectral Region
($\lambda < 100\text{Å}$)

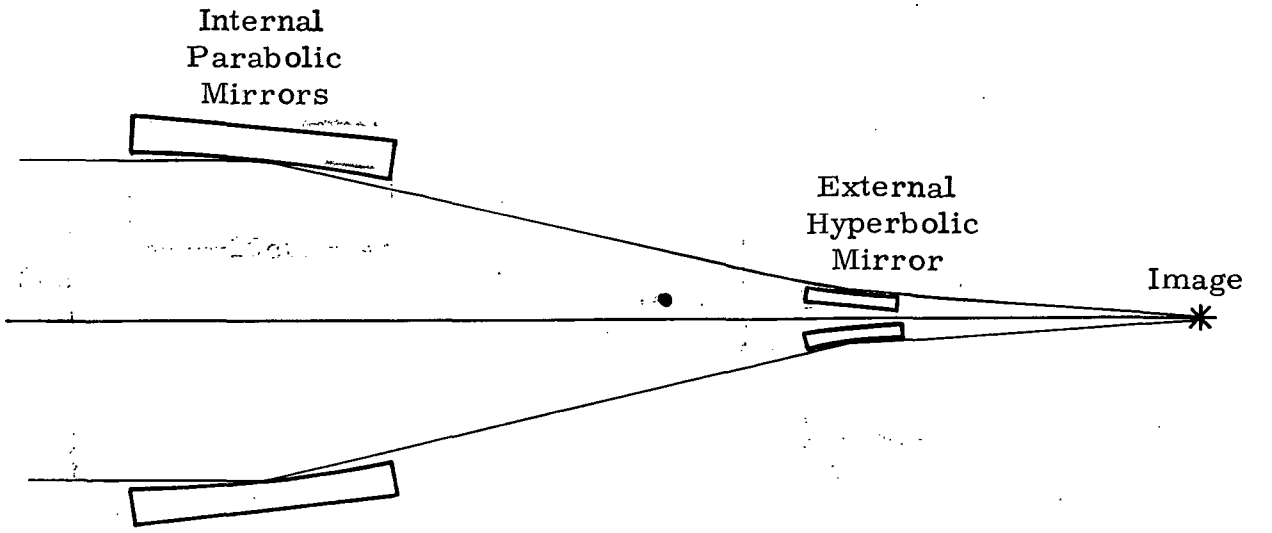

(b) Type II Wolter Telescope
For Extreme Ultra-Violet Spectral Region
($100\text{Å} < \lambda < 1000\text{Å}$)

Figure 1. Schematic Representation of Wolter Telescope Configurations

coating consisted of approximately 150 to 200Å of chromium acting as a binder film followed by 300 to 400Å of nickel to provide optimum X-ray reflectivity in the region of interest.

Since metalization by sputtering produces hard durable coatings, the feasibility of sputter deposition of various metallic coatings onto X-ray and extreme U.V. optical elements has been investigated. This program consisted of the following tasks which are described in Section II of this report.

- An analytical effort to predict the coating thickness distribution for both internal and external Wolter optical elements when vacuum evaporation or resistive heating (point sources) or sputtering (extended source) techniques are utilized.

- Fabrication of sputtered metal samples onto GFE substrates (using both hot and cold depositions) for subsequent extreme U.V. reflectivity measurements by GSFC.

- Investigation of the feasibility of sputter deposition techniques for the metalizing of internal and external X-ray and extreme U.V. reflectors.

The analytical investigation consisted of extending the present distribution codes developed for point vapor sources to the more general case of an extended source. This analysis showed, in general, that distribution errors would be reduced to negligible proportions by the correct use of aperture masks and by rotating and translating the cylindrical optical element over the vapor source.

The fabrication of metalized samples by sputter deposition included the preparation of films of nickel, molybdenum, ruthenium, and iridium deposited at ambient temperature and 300°C in two thicknesses (200Å and 1000A). These materials showed good adhesion to the substrate and all coated samples passed the Scotch Tape test. These coated samples were supplied to GSFC for reflectivity measurements, together with witness coatings deposited onto fused silica substrates, for film thickness and adhesion testing.

SECTION II

TECHNICAL DISCUSSION

COATING THICKNESS DISTRIBUTION ANALYSIS FOR WOLTER TELESCOPE ELEMENTS

The coating distribution for optical elements of any shape can be calculated from purely geometrical considerations by assuming that the film thickness deposited, dT, after a time dt is given by

$$dT\alpha = R \frac{\cos \quad \cos}{r^2} \, dt \qquad (1)$$

where r is the distance between source element dS and substrate element dA, α, is the angle of emission from the source, β is the angle of incidence on the substrate and R is the evaporation rate constant. In practice, the evaporation constant can change with time due to source depletion, and changes in the vapor angular distribution can occur as material is continuously evaporated. Equation (1) assumes a Lambertian vapor distribution which is also not always found in practice; however, vapor distribution can be modeled by replacing $\cos\alpha$ by $(\cos\alpha)^P$ where the value of p is obtained from experimental data.

Since the optical coating thickness is measured by quartz crystal thickness monitors during deposition, temporal changes in evaporation rate R are not included in the analysis. Lambertian source characteristics were also assumed at this stage since measured distributions for metallic vapor sources were not available.

For exterior deposition, the source is located ourside the substrate and directed toward the substrate axis, while interior deposition requires that the source be placed on the substrate's axis with its normal perpendicular to the axis. To achieve maximum film thickness uniformity for these sources, positions, and orientations, it is evident from the resulting geometric

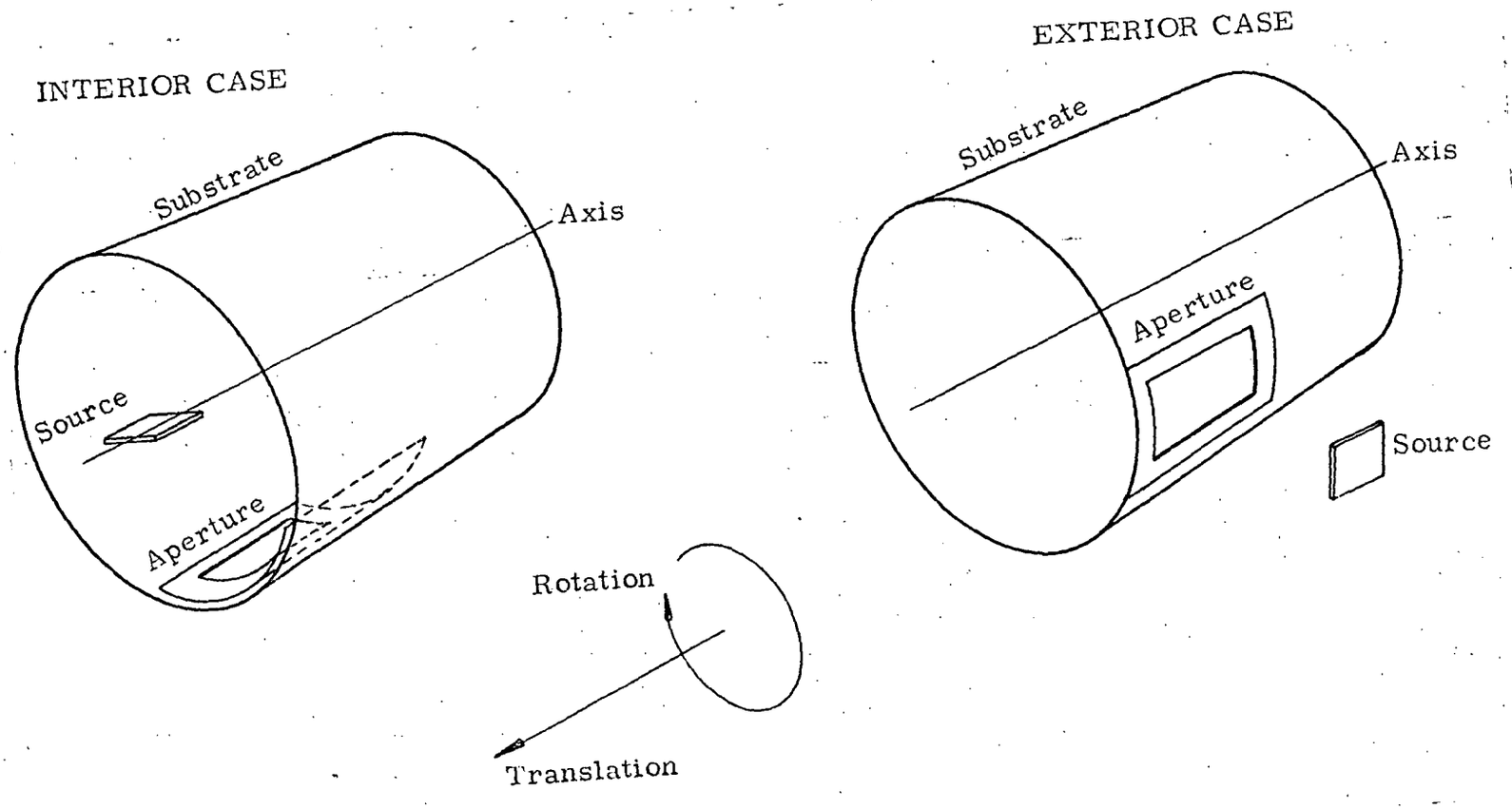

Figure 2. Deposition Configuration for Coating Interior and Exterior Cylindrical Surface

symmetries that the substrate should be rotated about and translated along its axis during deposition (see Figure 2). Uniformity is further improved when α and β are bounded by a rectangular aperture placed between the source and substrate. If the aperture is held stationary with respect to the source, points on the substrate will receive vapor only as they periodically achieve values of α and β encompassed by the aperture.

Another means for improving deposition uniformity becomes evident if Wolter substrates are viewed as truncated cones. This is a simplification made valid by the nearly constant slope of conic functions away from their vertices. To correct for the linear variation in radius along the cone's axis, an aperture tapered in width (dimension across the axis) is placed between the rectangular aperture and the substrate and translated with the substrate. Its maximum width is the width of the rectangular aperture and is at the cone's wide end for interior deposition and at its narrow end for exterior deposition. Film thickness variations now reduce to those on a cylindrical surface.

Two Fortran programs for use on an available IBM 370/158 were written to determine vapor deposition variations on a cylindrical surface arising from a rectangular source (optionally of zero extent) whose emissions reach the cylinder only through a rectangular aperture. Both source and aperture are assumed to be symmetrically oriented with respect to a cross-sectional radius of the cylinder, termed the Y-axis. The z-axis coincides with the cylinder axis, and the X-axis is chosen so that $\hat{X} \times \hat{Y} = \hat{Z}$ in the right-handed convention. One program covers deposition on the interior (concave) surface of the cylinder, while the other is concerned with deposition on its exterior (convex) surface (see Figure 3). Note that the exterior problem reduces to that of the interior when $h = -R$.

The parameters defined in Figure 3, together with a maximum permissible value for β and the source length, are read by each program to determine the aperture length. A maximum value for β is assumed to occur between source and aperture points that are diagonally opposed with respect to the Y-axis.

EXTERIOR CASE

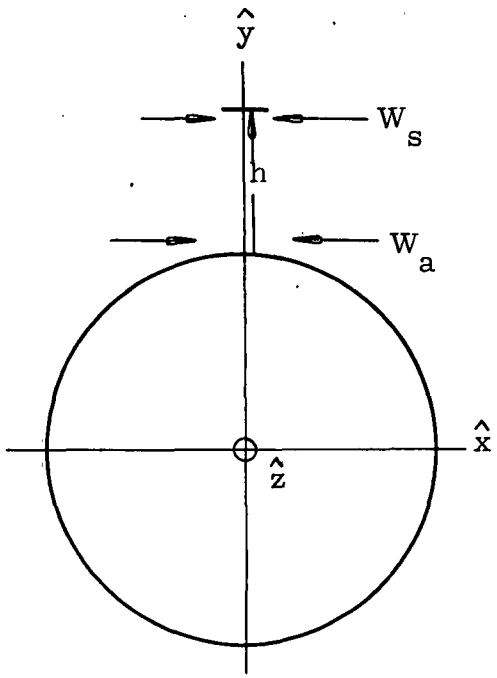

INTERIOR CASE

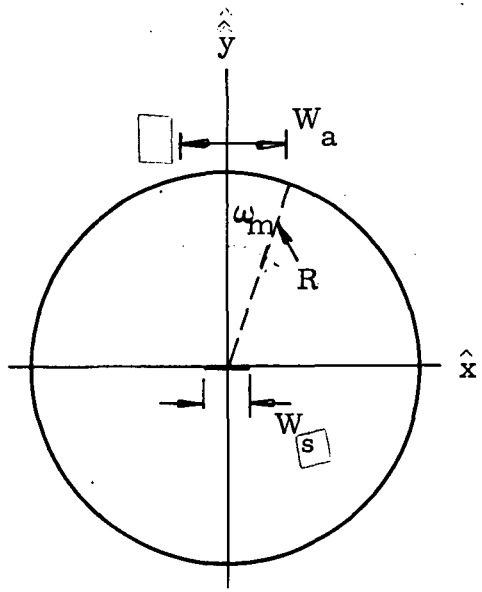

W_a = aperture width

W_s = source width

R = cylinder radius

ω_m = semi-angle of rotation for deposition cutoff

$$= \sin^{-1}\left(\frac{W_a}{2R}\right)$$

h = distance from cylinder to source ($h = -R$ for internal deposition)

Figure 3. Coating Deposition Geometries for Cylindrical Surfaces

Although this is quite valid for the exterior case, it is not rigorously so for the cylinder's interior. As will become evident later, however, this calculation need not be precise, and the assumption is therefore well made for both cases. For the determination of the aperture length from the program's input parameters, see Appendix A.

As the cylinder rotates and translates, each point on its surface traces its own helical path past the vapor source. In general, each point makes two or more passes through the aperture during which vapor deposits build up. These passes are separated by a distance A, the cylinder advance in z per revolution. Figure 4 illustrates such a series of passes. Note that the aperture length has been reduced from its calculated value to one integrally divisible by A. This practice makes the helix shown correspond to a cylinder point receiving minimal vapor deposits by virtue of the maximal α and β values it attains within the aperture. Since at any instant in time all points lying on this helix will also receive the same amount of material, the corresponding metallic film thickness is assigned a value of unity to which all other thicknesses are referred and the helix is consequently termed the normalizing helix. The normalizing thickness value is calculated by numerical integration of

$$\square \frac{\cos\alpha \cos\beta}{r^2}$$

over the source area for every point on the normalizing helix within the aperture. To calculate thickness values at all other cylinder points, the entire normalizing helix is shifted an increment in z and integrated as before. When the increment attains a value equal or greater than A, all cylinder points have been evaluated, each helical integration representing the thickness not at one, but rather at a whole family of points. Source points evaluated during integration are selected by the program input parameter ds as shown in Figure 5. A ds of zero treats the source as a point. Values for α and β are calculated according to Appendix B for the exterior case and according to Appendix C for the interior case.

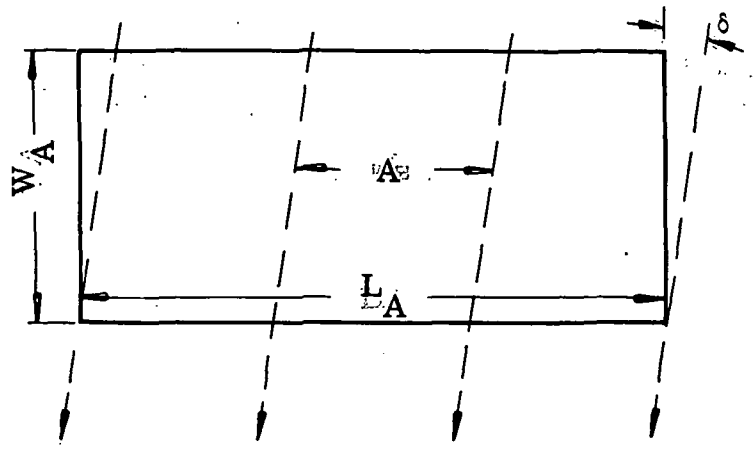

$$\frac{\delta}{2\omega_m} = \frac{A}{2\pi}$$

$$\delta = \frac{A \cdot \omega_m}{\pi}$$

Figure 4. Helical Path of a Point Due to Cylinder Rotation and Translation

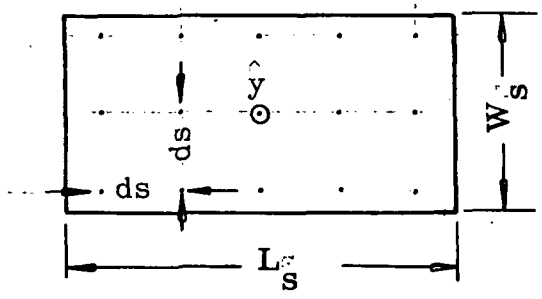

15 Source Points are evaluated for each helix point within the aperture in this example

Figure 5. Source Points Evaluated

The thickness associated with each helix of integration may be plotted against the z position of each helix relative to the normalizing helix. This spatial thickness function has a period of A in z. If the helix traced by a given point is mapped onto the cylinder so as to pass through that point, it becomes a control of equal film thickness on the cylinder. Recall that all cylinder points on any helix must possess the same helix of integration. A representation of this mapping process is displayed in Figure 6.

COMPUTED DISTRIBUTIONS FOR INTERNAL AND EXTERNAL CONFIGURATIONS

A number of computer runs were made with each program to explore the effect of varying source dimensions on vapor deposition variations. The results of this experiment for exterior and interior cylinder surfaces representative of typical Wolter substrates appear in Figures 7 and 8, respectively. No source tested gave rise to a thickness variation greater than 0.5 percent. If a film thickness of 1000Å is deposited on a substrate, a modulation in thickness of less than 5Å would be expected. A value of 1.0 inch for A yields a maximum deviation from the desired surface slope of about 6×10^{-8} radian (see Appendix D), assuming changes in film thickness to be a sinusoidal function of z distance. It is worth noting that changes to the source width have little effect on thickness variations in the interior case. This is a direct result of the cylinder's interior normal always pointing at the Z-axis, where the source lies. Position variations in the X direction, therefore, have only minor effects upon β. Since the source lies nowhere near the Z-axis in the exterior case, thickness variations are comparatively sensitive to source width changes.

An effort to produce deposition geometries resulting in minimal deposition variations will require a more extensive exploration of program input parameters than that has been made to date. For example, a further restriction of β's maximum attainable value from 30° to 20° should reduce deposition variations correspondingly. With the techniques and intuition developed in this study, the surface figure of both type 1 and type 2 Wolter substrates can be maintained within several angstroms during application of a reflective film.

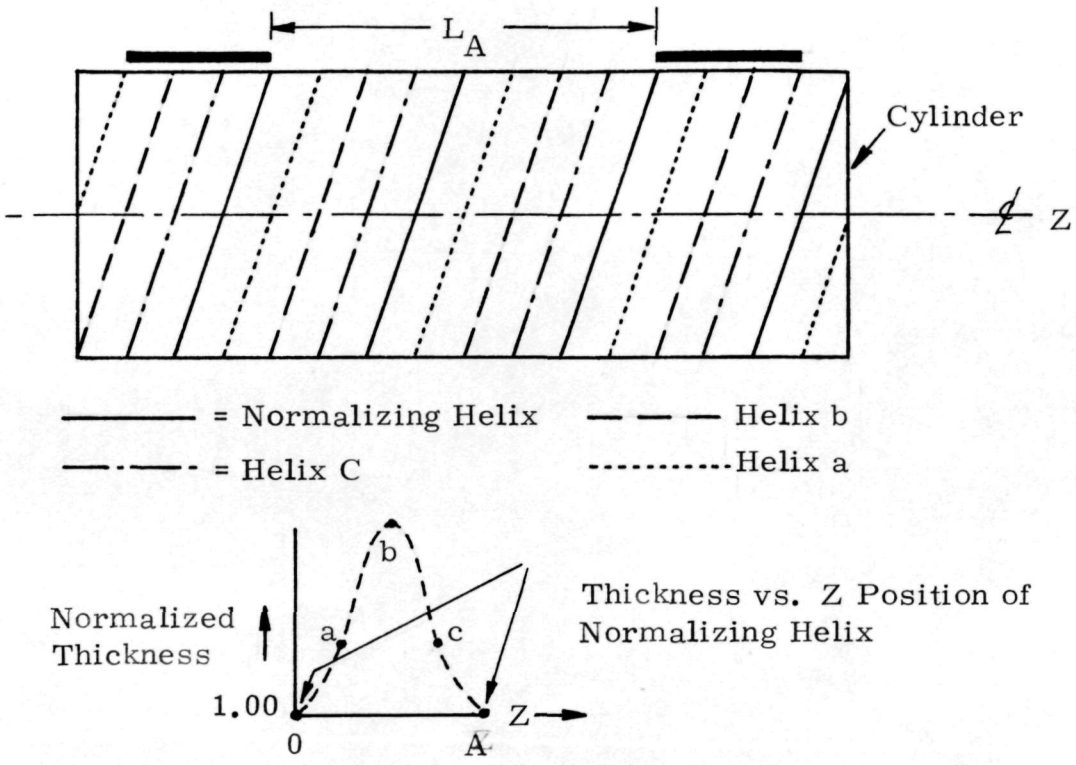

Helices of Integration Mapped Onto Their Corresponding Cylinder Points

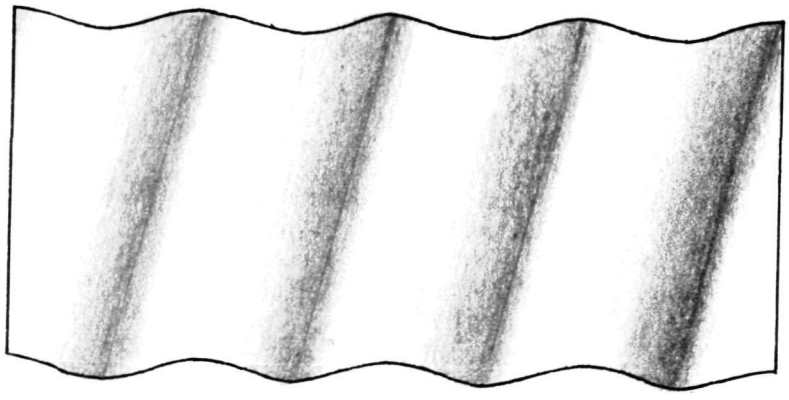

Coated Cylinder Thickness Variations (Greatly Exaggerated) Seen as Illuminated From Left

Figure 6. Representation of Mapping Process

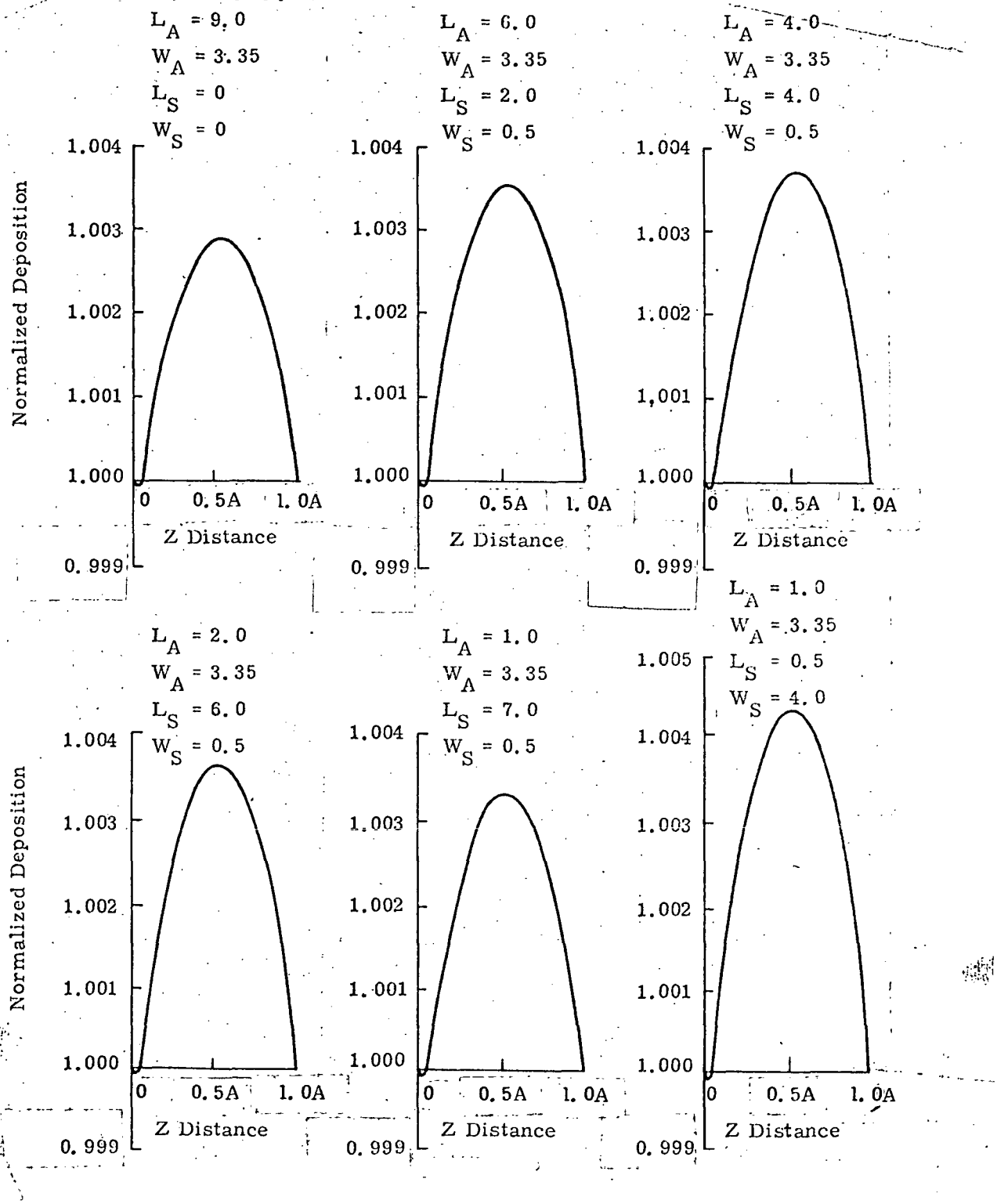

Figure 7. Relative Vapor Distribution on Convex Cylinders from an Extended Source (R = 10, dzA = 1.0, maximum allowable β = 30°, ds = 0.8, h = 10) (All dimensions are in inches)

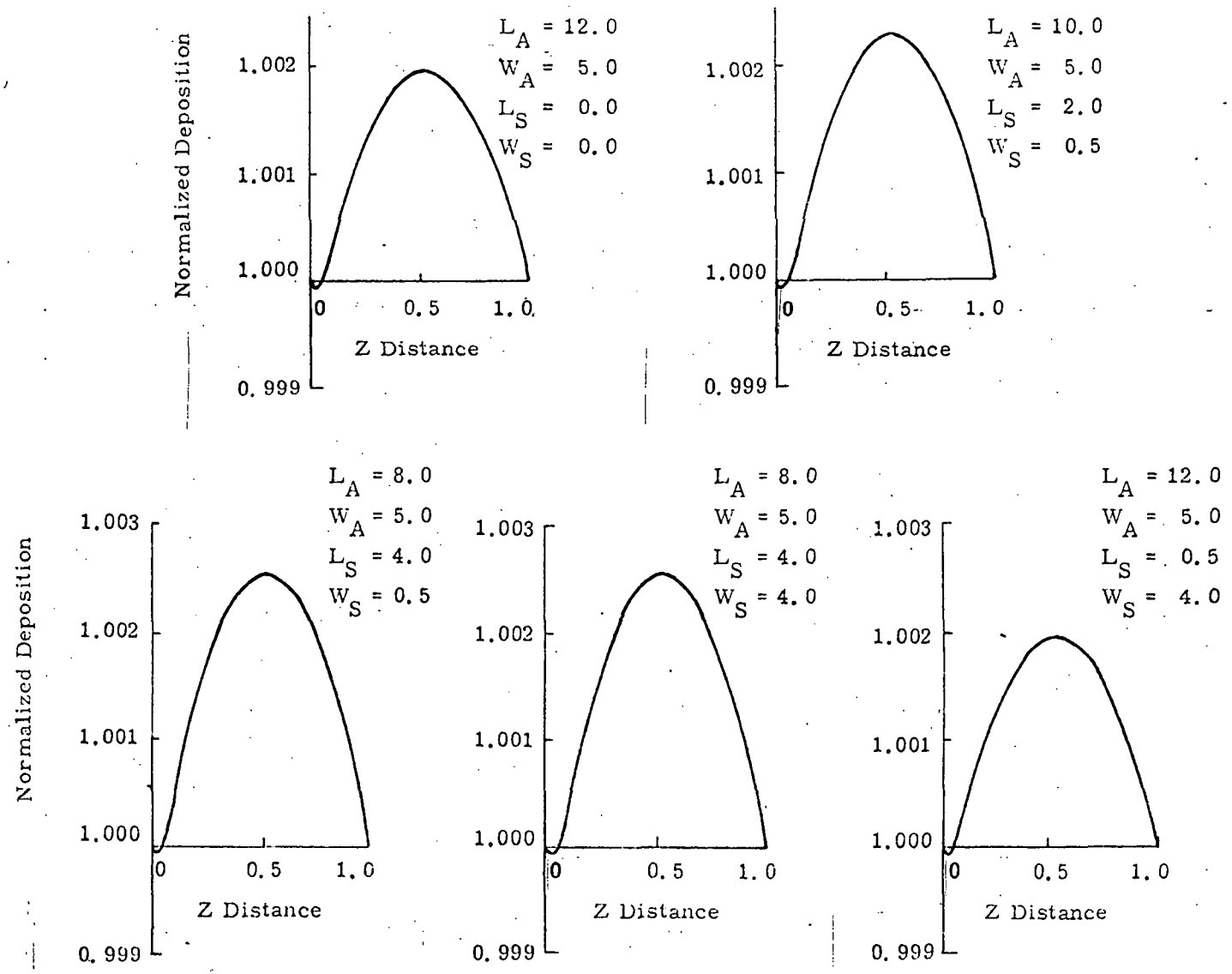

Figure 8. Relative Vapor Deposition on Concave Cylinders from Extended Sources (R = 11.0, dzA = 1, maximum allowable β = 30°, ds = 0.8) (All dimensions are in inches)

SPUTTERED FILM METALIZING - SAMPLE PREPARATION

A matrix of sputtered metal coatings was prepared according to Table 1 where the various metals were deposited onto polished substrates (GFE) of fused silica, Cervit and polished electroless nickel. Film thicknesses of 200A or 1000A were deposited at two temperatures, 40°C and 300°C, and witness samples of fused silica were prepared during each sputter cycle.

CLEANING PROCEDURES

All GFE substrates and fused silica witness pieces were cleaned prior to sputtering using the following procedures:

Cervit and Fused Silica Cleaning Procedure

(1) Rinse in distilled water.

(2) Clean with cotton swab and mixture of Orvus (a non-aromatic detergent) and distilled water.

(3) Rinse and swab with wet cotton and snowfloss (hydrated amorphous silica).

(4) Rinse with Orvus.

(5) Rinse with dionized water.

(6) Rinse with hot nanograde alcohol.

Nickel Cleaning Procedure

(1) Pour Mr. Clean on surface and let stand.

(2) Swab gently with cotton.

(3) Clean threaded holes with Q-tip and Mr. Clean.

(4) Rinse with dionized water.

(5) Blow dry with filtered nitrogen.

TABLE 1

SPUTTERED METAL/SUBSTRATE COMBINATIONS DEPOSITED AT 40°C AND 300°C

	Ambient Temperature (Cold Deposition ~ 40°C) Film Thickness (Å)		High Temperature Deposition (Temp = 300°C ± 20°C) Film Thickness (Å)	
Sputtered Film	200Å	1000Å	200Å	1000Å
Nickel	FS	FS	FS	FS
		CV		
		NI		
Molybdenum	FS	FS	FS	FS
	CV			
	NI			
Ruthenium	FS	FS	FS	FS
				CV
				NI
Iridium	FS	FS	FS	FS
			CV	
			NI	

Substrate Code

FS = Fused Silica Substrate (Polished)

CV = Cervit Substrate (Polished)

NI = Nickel Substrate (Polished)

SPUTTERING TARGET FABRICATION

All targets were obtained in the form of 6-inch diameter disks of material bonded to a copper backing plate. The molybdenum target was provided by Perkin-Elmer and the nickel, iridium, and ruthenium targets were obtained from Sylvania. Considerable difficulty was experienced by Sylvania in providing a metal bonded ruthenium target and the target specifications were changed to allow the bond to be made using Epo Tek 4159-silver epoxy (non-outgassing). The completed target was vacuum baked for 4 hours at 300°C after bonding and preheated and outgassed in vacuum at Perkin-Elmer before use.

SPUTTER GEOMETRY

The sputter geometry utilized for the preparation of all metal samples is shown in Figure 9. Two fused silica witness pieces 2 inches in diameter and one 2-inch x 2-inch GFE mirror sample are placed in cutouts in an alumin mask to ensure that all surfaces are equidistant from the surface of the sputtering target. A step coating is produced on the two circular samples, by means of a shadow bar, to enable coating thickness to be determined.

Hot depositions were carried out using the substrate holder placed upon a heater block consisting of a nichrome heater embedded in ceramic. Both substrate and mask could be heated to 300°C to 400°C using this configuration and sputter deposition was carried out with the heater turned off. The temperature of the substrate holder was monitored during deposition by a thermocouple embedded in the aluminum mask and showed a low temperature decay rate (~ 1°C per minute).

Since it wouldbe impractical to utilize sputter etching or bias sputtering during the metalization of an X-ray optic, these techniques were not utilized during the preparation of the coating samples.

FIG 8

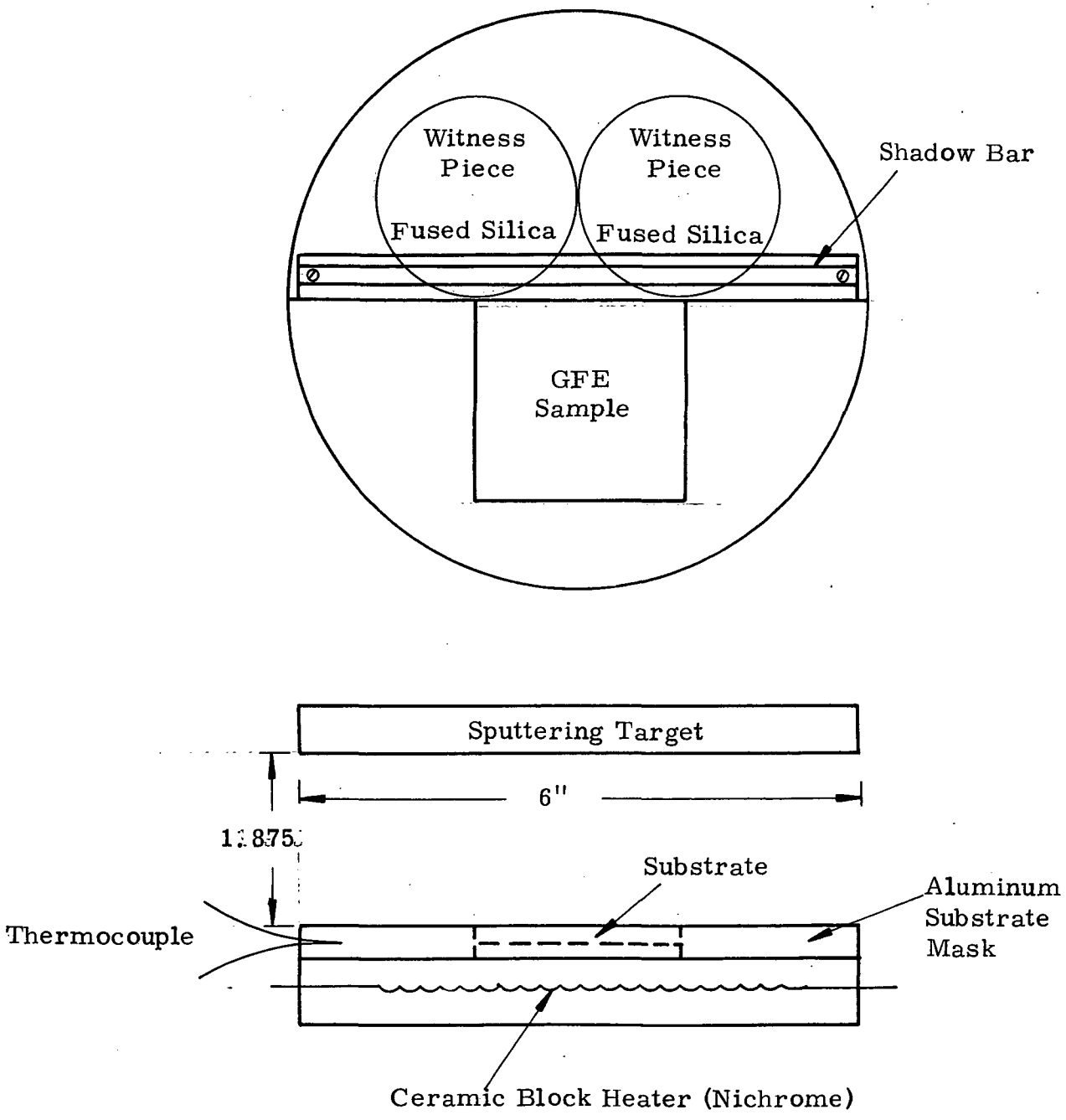

Figure 9. Sputtering Geometry For Cold and Heated Depositions

FILM EVALUATION

The sputtered films were deposited in two thicknesses after system thickness calibration runs were completed, and thicknesses were measured using a Sloan Angstrometer and a FECO interferometer. Subsequent to deposition all films were tested for adhesion using the Scotch Tape test.

SPUTTERED SAMPLE DATA

The deposition conditions, including temperature, gas pressure, base pressure, sputter power and sputter time were recorded for each sample and are given for the four different metals in Tables 2 through 5. All deposited films showed excellent adhesion on the fused silica witness piece and passed the Scotch Tape test.

METALIZATION OF CYLINDRICAL X-RAY TELESCOPE ELEMENTS

X-ray telescope elements for the HEAO-B space vehicle, consisting of internal parabolas and hyperbolas, were metalized with a film layer of chrome/nickel using a vacuum chamber modified to allow the optical element to rotate and translate over the vapor source. The coating configuration is shown in Figure 10 where the optic to be coated is mounted inside a mirror frame assembly which rotates inside a translating carriage. The vapor sources consist of electron beam guns mounted from one end of the chamber along the axis of the optical element. The coating distribution can be controlled by the choice of a stationary coating mask together with the rotary and translational motion of the optical element. A horizontal coating chamber has been modified for this purpose (Figure 11) and was successfully utilized to coat the internal surfaces of the HEAO-B telescope assembly optics. Table 6 shows the measured variations in coating thickness and surface roughness obtained from six witness samples covering the entire length of one rotational meridian for each of six telescope elements. The mean variation in coating thickness achieved is near 10%.

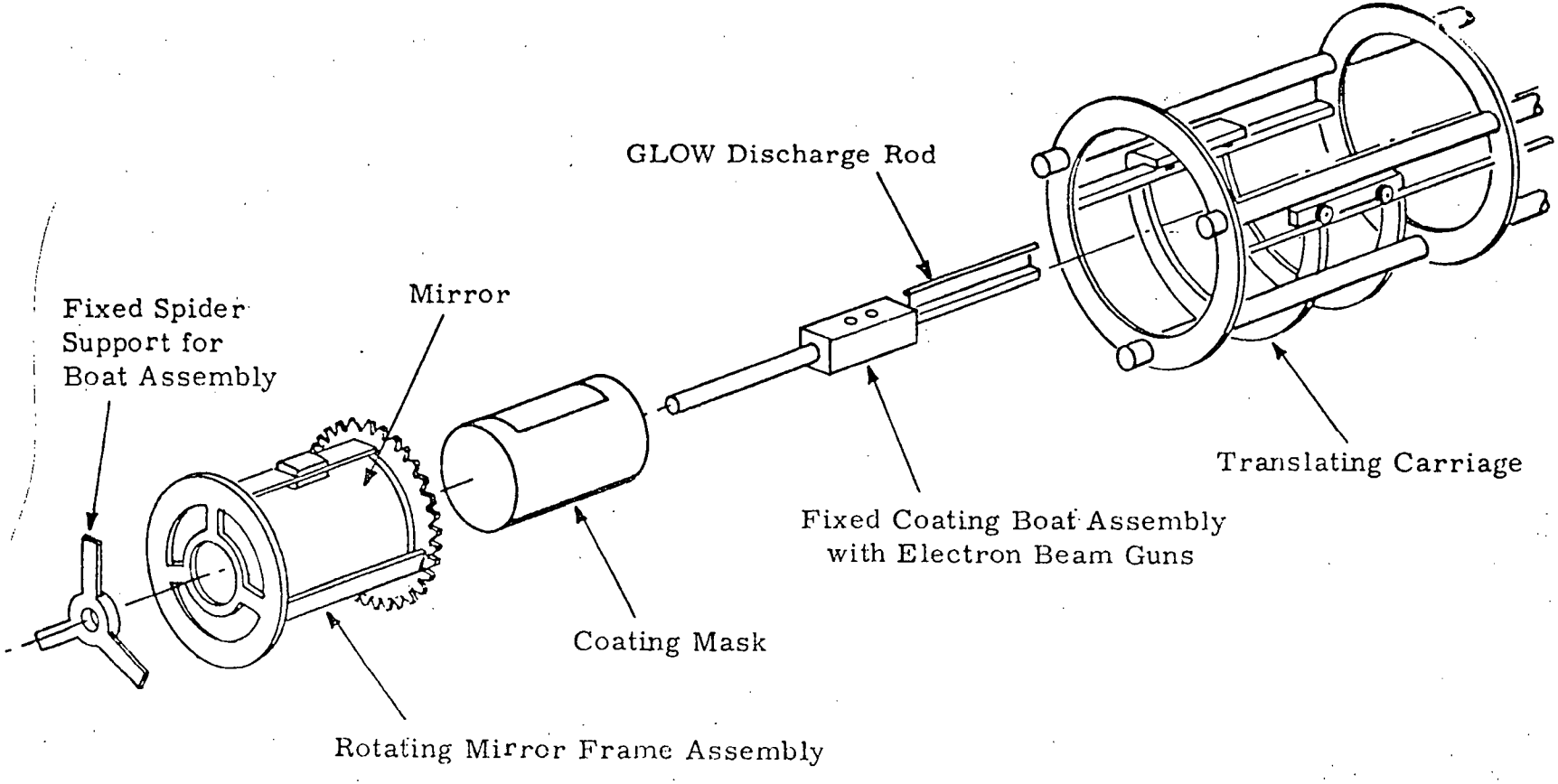

Figure 10. Coating Configuration for Internal Wolter Type Reflectors

Figure 11. Horizontal Coating Chamber Modified to Enable Mirror to Rotate and Translate Over a Fixed Coating Mask and Electron Beam Gun Vapor Source

TABLE 2. SPUTTERED MOLYBDENUM SAMPLE DATA

Substrate/ Witness Code	Deposition Temperature (°C)	Thickness (A)	Gas Pressure (Argon) (μm)	Power (watts)	Time (min)	Base Pressure (torr)	Scotch Tape of 2nd Witness
MOFS-1A	40	216	20	50	2.8	4.3×10^{-7}	Passed
MOFS-2	40	1066	20	50	14.0	6.7×10^{-7}	Passed
MOCT-3	40	166	20	50	2.8	5.7×10^{-7}	Passed
MONI-4	40	177	20	50	2.8	6.0×10^{-7}	Passed
MOFS-5	300	850	20	50	13.0	9.0×10^{-7}	Passed
MOFS-6 A	300	309	20	50	2.5	8.6×10^{-7}	Passed

Code	
Molybdenum	MO
Fused Silica	FS
Cervit	CT
Nickel	NI

TABLE 3. SPUTTERED NICKEL SAMPLE DATA

Substrate/ Witness Code	Deposition Temperature (°C)	Thickness (Å)	Gas Pressure (Argon) (μm)	Power (watts)	Time (min)	Base Pressure (torr)	Scotch Tape of 2nd Witness
NIFS-1	40	206	20	50	2.25	3.7×10^{-7}	Passed
NIFS-2	40	1081	20	50	11.2	3.3×10^{-7}	Passed
NICT-3	40	1082	20	50	11.2	3.5×10^{-7}	Passed
NINI-4	40	1033	20	50	11.2	5.2×10^{-7}	Passed
NIFS-5	300	981	20	50	11.76	3.8×10^{-7}	Passed
NIFS-6	300	231	20	50	3.10	5.4×10^{-7}	Passed

Code

Substrate		Film	
Nickel	NI	Molybdenum	MO
Fused Silica	FS	Nickel	NI
Cervit	CT	Iridium	IR
		Ruthenium	RU

TABLE 4. SPUTTERED RUTHENIUM SAMPLE DATA

Substrate/ Witness Code	Deposition Temperature (°C)	Thickness (Å)	Gas Pressure (Argon) (μm)	Power (watts)	Time (min)	Base Pressure (torr)	Scotch Tape of 2nd Witness
RUFS-1	40	255	20	50	3.27	5.2×10^{-7}	Passed
RUFS-2	40	1049	20	50	10	4.1×10^{-7}	Passed
RUFS-3	300	206	20	50	2.46	7.8×10^{-7}	Passed
RUFS-4	300	967	20	50	10	6.8×10^{-7}	Passed
RUCT-5	300	1017	20	50	10	6.0×10^{-7}	Passed
RUNI-6	300	981	20	50	10	8.3×10^{-7}	Passed

Code

Substrate		Film	
Nickel	NI	Molybdenum	MO
Fused Silica	FS	Nickel	NI
Cervit	CT	Iridium	IR
		Ruthenium	RU

TABLE 5. SPUTTERED IRIDIUM SAMPLE DATA

Substrate/ Witness Code	Deposition Temperature (°C)	Thickness (Å)	Gas Pressure (Argon) (μm)	Power (watts)	Time (min)	Base Pressure (torr)	Scotch Tape of 2nd Witness
IRFS-1	40	199.9	20	50	1.98	4.8×10^{-7}	Passed
IRFS-2	40	987.0	20	50	8.76	6.2×10^{-7}	Passed
IRCT-3	300	222.0	20	50	1.98	7.2×10^{-7}	Passed
IRFS-4	300	247.0	20	50	1.98	4.6×10^{-7}	Passed
IRNI-5	300	222.0	20	50	1.98	5.2×10^{-7}	Passed
IRFS-6	300	1071.0	20	50	8.76	4.1×10^{-7}	Passed

Code

Substrate		Film	
Nickel	NI	Molybdenum	MO
Fused Silica	FS	Nickel	NI
Cervit	CT	Iridium	IR
		Ruthenium	RU

TABLE 6. MEAN AND STANDARD DEVIATION IN COATING THICKNESS AND SURFACE ROUGHNESS OF WITNESS SAMPLES FOR SIX X-RAY TELESCOPE ELEMENTS

Chamber Config. For HEAO-B Element	Thickness (Å)	Surface Roughness (RMS) Uncoated (Å)	Coated (Å)	Percent Thickness Variation
P-1	780±31	22±2	21±2	7.95
P-3	1101±43	32±3	30±3	7.81
P-4	927±8	24±4	23±4	10.36
H-6	953±40	28±5	26±5	8.39
H-7	1043±84	25±5	19±5	16.11
H-8	1146±66	18±4	18±5	11.52

The mean percentage thickness variation for all 6 sets of witness samples is 10.36±3.2.

The optical coating for the small hyperbola that requires its outer surface to be metalized is a much simpler coating task than is that for the larger elements. Recently, hard multilayer dielectric coatings have been deposited onto the outer surface of an elliptical cylinder for use as the flashlamp cavity for a YAG laser. This type of coating (a 27-layer dichroic) was deposited onto the outer surface as 150°C by rotating the cylinder over a stationary slit mask and electron beam gun source in vacuum. The finished coated cylinder is shown in Figure 12.

It should be possible to configure a sputter target in the form of a cylinder of the same length as the X-ray optic but several inches less in diameter. This target could be placed coaxial with the optic to be coated and RF sputtering could be performed in the conventional manner. However, this approach is not recommended for large optical surface elements since the use of a sputtering target in this form using metals such as iridium or ruthenium would be prohibitively costly. In addition, the power requirements ($\sim 10^4$ watts) would be exceedingly large because of the large surface area of the target. The use of a hollow target for the small hyperbola (5 cm dia.) is a possible alternative sputtering configuration since target costs should not be excessive unless target bonding becomes a problem.

Sputter metalization of the large X-ray optical elements can be carried out economically by replacing the present electron beam vapor source by a plane sputter target. The most obvious difference between this scheme and conventional sputtering is the large throw distance between target and substrate which will produce a lower deposition rate due to the inverse square law decrease in vapor density. Commercial sputtering masks are available that presently sputter aluminum at 10Å/second at a 20-inch throw distance so that rates of 1 to 3Å/second should be attainable for metals such as nickel, molybdenum, ruthenium and iridium.

A more important consideration sputter deposition is the adhesion of the film to the substrate and this is somewhat dependent upon the surface temperature produced by electron bombardment during the sputter process. For large throw distances and consequently low sputter rates, the surface of a large optical element may not rise to the temperatures normally achieved

Figure 12. Multilayer Dichroic Coating Deposited onto the Outer Surface of an Elliptical Cylinder (Approximately 3 inches long and 2 inches in diameter)

in conventional sputtering and it may be necessary to heat the substrate externally prior to deposition. External heating using quartz iodine lamps or Calrod heaters can be used to provide temperatures in the 200° C to 300° C range; however, the effect of this heat cycle upon the roundness of an X-ray optical element fabricated from fused silica is not known. Such temperatures are not expected to affect the roundness of fused silica optics although experimental measurements using cutoff sections of X-ray telescopes should be made before any hot sputter depositions are attempted on actual elements.

SECTION III

SUMMARY

The investigation of Sputter Metalization of Wolter Type Optical Elements can be summarized as follows:

- An analytical task has shown that the coating thickness distribution for both internal and external optical elements coated using either electron beam resistance, or sputter sources can be made very uniform and well not affect the surface figure of the coated elements.

- Sputtered samples of nickel, molybdenum, iridium, and ruthenium deposited once both hot (300°C) and cold substrates (40°C) show excellent adhesion. Such sputtered deposits onto fused silica witness pieces all passed the Scotch Tape tests and it is assumed that equivalent adhesion is obtained on the GFE samples of Cervit and nickel.

- Comparison of Table 6 data with results of the analytical computer study indicates potential for improvement in the deposition of uniformly thick films on substrates with cylindrical symmetry. The computer coding now available should aid in selection of optimal geometries and design of more effective coating masks in the future. It is also valid for the extended sputtering sources able to deposit highly durable reflective coatings. A series of fused silica cylinders might be sputter coated on both interior and exterior surfaces with an etlon composed of opaque silver overlaid by films of $S:O_2$ and of silver with a 2% transmission factor visible wavelengths. Such a coating can then be used to evaluate the film thickness uniformity brought about by the sputtering configuration employed. Following coating, each cylinder is cut parallel to its axis into a set of strips. When placed under an available FECO (Fringes of Equal Chromatic Order) interferometer; thickness variations as small as 10A in the

etalon will become readily visible in the interference pattern generated. This technique has already been utilized with success on an axicon coated with an Ag (opaque)/ThF4/Ag (2% transmission) etalon. An improvement in the final coated surface roughness in Table 6 might be realized in experiments to polish a surface after a sputtered film has been applied.

REFERENCES

1. J.D. Mangus, J.H. Underwood, Appl. Opt. 8, 95 (1969).

2. J.D.Mangus, Appl. Opt. 9, 1019 (1970).

3. HEAO-B X-RAY Telescope Final Technical Report No. 13292, Perkin-Elmer Corporation, 17 Jan. 1977.

APPENDIX A

DETERMINATION OF APERTURE LENGTH (LA)

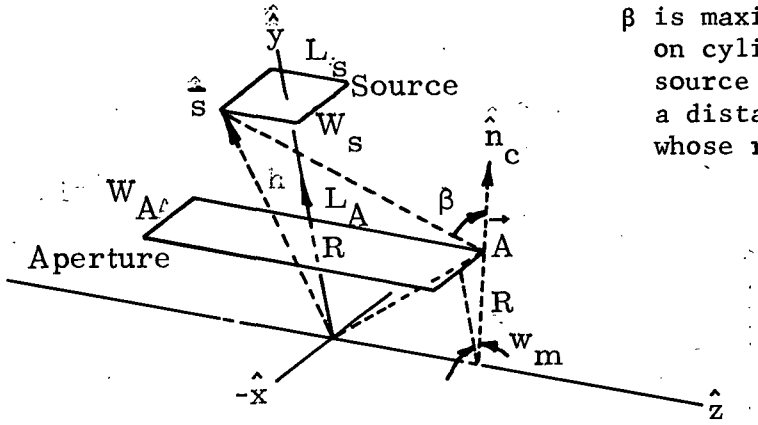

β is maximum angle of incidence on cylinder at point A from source point S. The source is a distance $h\hat{y}$ from the cylinder, whose radius is R.

The following equations are obtained from the coating geometry illustrated above

$$\cos\beta = \frac{\vec{AS}\cdot\hat{n}_c}{|\vec{AS}|}$$

$$\hat{n}_c = \sin\omega_m\,\hat{x} + \cos\omega_m\,\hat{y}$$

$$\vec{A} = \frac{W_a}{2}\,\hat{x} + R\cos\omega_m\,\hat{y} + \frac{L_a}{2}\,\hat{z}$$

$$\vec{S} = -\frac{W_s}{2}\,x + (R+h)\hat{y} - \frac{L_s}{2}\,\hat{z}$$

$$\vec{AS} = \vec{S}-\vec{A}$$

$$\vec{AS} = -\left(\frac{W_s + W_a}{2}\right)\hat{x} + (R+h - R\cos\omega_m)\hat{y} - \left(\frac{L_s + L_a}{2}\right)\hat{z}$$

$$\cos\beta = \left[-\sin\omega_m\left(\frac{W_s + W_a}{2}\right) + \cos\omega_m\,(R+h - R\cos\omega_m)\right]\left[\frac{(W_s + W_a)^2 + (L_s + L_a)^2}{4} + (R+h - R\cos\omega_m)^2\right]^{-\frac{1}{2}}$$

34

Solving for L_a, we have

$$L_a = \frac{-b+\sqrt{b^2-4ac}}{2a}$$

where:

$$a = \frac{\cos^2\beta}{4}$$

$$b = \frac{L_s \cdot \cos^2\beta}{2}$$

$$c = \left[\cos^2\beta \frac{(W_s + W_a)^2 + L_s^2}{4} + (R+h - R\cos\omega_m)^2\right] - \left[\cos\omega_m(R+h - R\cos\omega_m) - \sin\omega_m \frac{W_s + W_a}{2}\right]^2$$

for the interior case, however, h = -R only and

$$c = \cos^2\beta\left[\frac{(W_s + W_a)^2 + L_s^2}{4} + R^2 \cos^2 \omega_m\right] - \left\{-R\cos^2\omega_m - \sin\omega_m \frac{W_s + W_a}{2}\right\}^2$$

APPENDIX B

EMISSION AND INCIDENCE ANGLES EXTERIOR TO CYLINDER

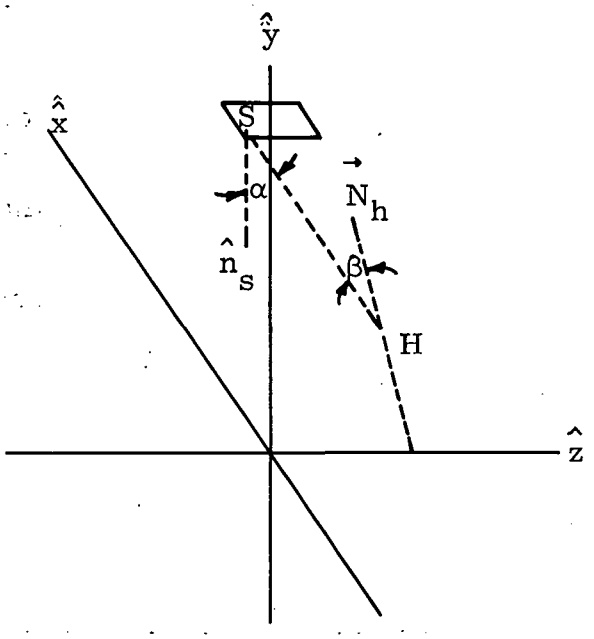

S is an arbitrary point on the source

H is an arbitrary point on the cylinder

$\hat{n}_s$ is unit normal to source surface

$\vec{N}_h$ is normal to exterior cylinder surface

Defining:

$$\vec{S} = X_s\hat{x} + Y_s\hat{y} + Z_s\hat{z}$$

$$\vec{H} = X_h\hat{x} + Y_h\hat{y} + Z_h\hat{z}$$

We have:

$$\hat{n}_s = X_s\hat{x} + (Y_s-1)\hat{y} + Z_s\hat{z} - \vec{S} = -\hat{y}$$

$$\vec{N}_h = \vec{H} - Z_h\hat{z} = X_h\hat{x} + Y_h\hat{y}$$

The source emission cosine factor is

$$\cos\alpha = \frac{\vec{SH}\cdot\hat{n}_s}{|\vec{SH}|} = \frac{Y_s - Y_h}{\left\{(X_h - X_s)^2+(Y_h - Y_s)^2+(Z_h - Z_s)^2\right\}^{\frac{1}{2}}}$$

The cylinder incidence angle cosine factor is

$$\cos\beta = \frac{\vec{HS}\cdot\vec{N}_h}{|\vec{HS}|\,|\vec{N}_h|} = \frac{X_h(X_s - X_h) + Y_h\,(Y_s - Y_h)}{R\left\{(X_s - X_h)^2+(Y_s - Y_h)^2+(Z_s - Z_h)^2\right\}^{\frac{1}{2}}}$$, R ≡ radius of cylinder

The instantaneous deposition on H from S is then proportional to

$$\frac{\cos\alpha\cdot\cos\beta}{R^2}$$

APPENDIX C

EMISSION AND INCIDENCE ANGLES INTERIOR TO CYLINDER

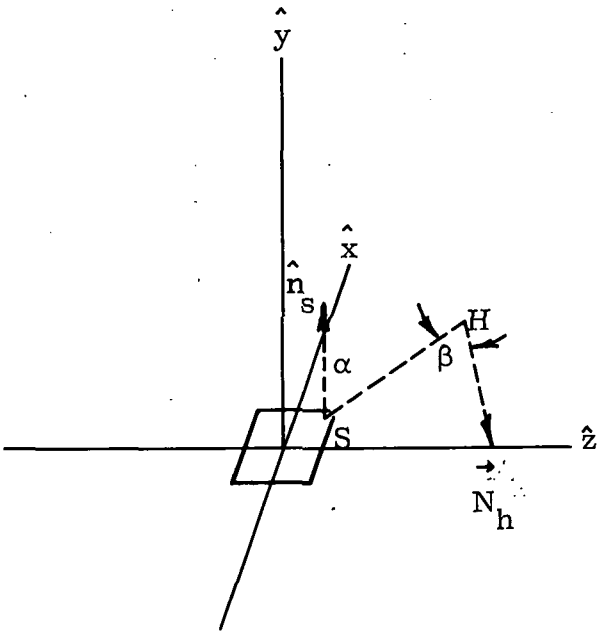

S is an arbitrary point on the source

H is an arbitrary point on the cylinder

$\hat{n}_s$ is unit normal to source surface

$\vec{N}_h$ is normal to interior cylinder surface

Defining:

$$\vec{S} = X_s\hat{x} + Z_s\hat{z}$$

$$\vec{H} = X_h\hat{x} + Y_h\hat{y} + Z_h\hat{z}$$

We have:

$$\hat{n}_s = X_s\hat{x} + \hat{y} + Z_s\hat{z} - \vec{S} = \hat{y}$$

$$\vec{N}_n = Z_h\hat{z} - \vec{H} = -X_h\hat{x} - Y_h\hat{y}$$

The source emission angle cosine factor is

$$\cos\alpha = \frac{\vec{SH}\cdot\hat{n}_s}{|\vec{SH}|} = \frac{Y_h}{\left\{(X_h - X_s)^2 + Y_h^2 + (Z_h - Z_s)^2\right\}^{\frac{1}{2}}}$$

The cylinder incidence angle cosine factor is

$$\cos\beta = \frac{\vec{HS}\cdot\vec{N}_h}{|\vec{HS}||\vec{N}_h|} = \frac{X_h(X_h - X_s) + Y_h^2}{R\left\{(X_s - X_h)^2 + Y_h^2 + (Z_s - Z_h)^2\right\}^{\frac{1}{2}}}$$, R ≡ radius of cylinder

The instantaneous deposition on H from S is then proportional to

$$\frac{\cos\alpha\cos\beta}{R^2}$$

37

APPENDIX D - PRESERVATION OF SUBSTRATE SURFACE FIGURE AFTER COATING

The "worst case" coating has the following deposition geometry:

A = 1.0 inch

maximum β = 30°

d_s = 0.8 inch

L_a = 1.0 inch

L_s = 0.5 inch

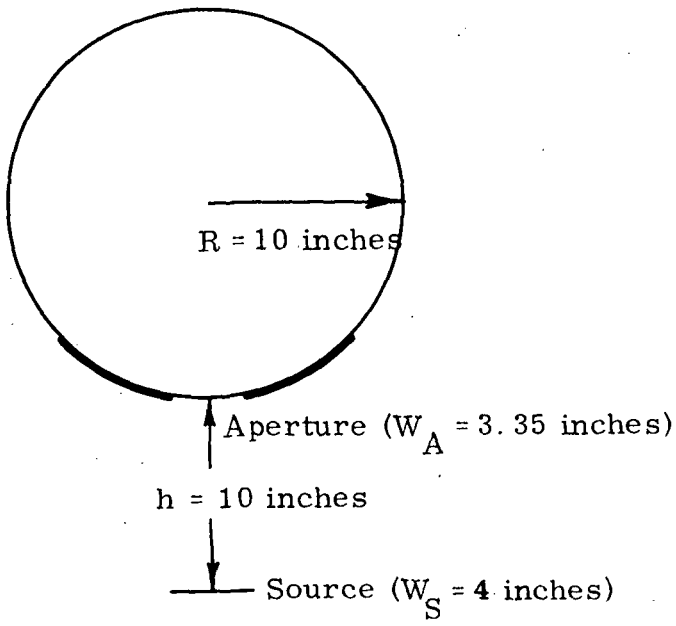

Assuming a total film thickness of 1000Å which varies by 0.5 percent, the peak-to-valley variation in thickness is 5Å. If this variation is a sinusoidal function of z distance (in inches), its value T (in Angstroms) is:

$$T = 2.5 \sin 2\pi z$$

Its slope is:

$$\frac{dT}{dz} = 5\pi \cos 2\pi z$$

The greatest departure from the desired slope is at z=o

$$\left.\frac{dT}{dz}\right|_{z=o} = 5\pi \text{ Angstrom/inch}$$

$$= 5\pi \cdot 10^{-10} \cdot 39.37 = 6.184 \cdot 10^{-8} \text{ radians}$$